Research Square

Preprints are preliminary reports that have not undergone peer review.
They should not be considered conclusive, used to inform clinical practice,
or referenced by the media as validated information.

Enhanced Structural, Optical, and Gas Sensing Performance of Cu-Doped SnO_2 Nanostructures for NO_2 and NH_3 Gases

J. F. Mohammad
University of Anbar
Ruaa H. Jasim
Al-Iraqia University
Abd alhameed A. Hameed
Ministry of Education, Education Direction in Al-Anbar
Bilal K. Al-Rawi
sc.bilal_alrawi@uoanbar.edu.iq

University of Anbar

Research Article

Keywords: SnO2-CuO films, NH3 gas sensor, NO2 gas sensor, spray pyrolysis, Thin films

Posted Date: April 24th, 2026

DOI: https://doi.org/10.21203/rs.3.rs-9053897/v1

License: This work is licensed under a Creative Commons Attribution 4.0 International License.
Read Full License

Additional Declarations: No competing interests reported.

Version of Record: A version of this preprint was published at Sensing and Imaging on May 28th, 2026.
See the published version at https://doi.org/10.1007/s11220-026-00810-x.

Abstract

In order to enhance their gas-sensing capabilities for NH_3 and NO_2, this study demonstrates the creation and assessment of pure SnO_2 and Cu-doped tin oxide (SnO_2:Cu) nanostructured thin films produced using the spray pyrolysis process. At 350°C, the films were formed on glass substrates with a precursor molar concentration of 0.02 M and copper doping ratios of 1%, 3%, and 5%. X-ray diffraction (XRD) research confirmed that there are no signs of secondary phases and that all films have a polycrystalline tetragonal rutile structure. The size of the crystallites decreased slightly as the Cu content rose. AFM and SEM investigations show that copper doping improved the effective surface area by increasing surface uniformity and significantly reducing grain size and surface roughness. EDS analysis demonstrated the effective copper assimilation and the lack of contamination. Due to quantum confinement effects, optical tests revealed that the direct band gap increased from 3.73 eV for undoped SnO_2 to 3.88 eV for 5% Cu-doped films. Hall effect results showed that the doping increased the quantity of carriers and that all of the films had n-type conductivity. The SnO_2 film containing 1% Cu performed the best, according to gas-sensing evaluations, with maximum sensitivities of 19.12% toward NH_3 and 96.14% toward NO_2 at an operating temperature of 200°C, as well as quick response and recovery times. These findings demonstrate that appropriate Cu doping may increase SnO_2 thin-film gas-sensing capabilities by increasing surface activity and p–n junction formation.

1. Introduction

The growth of the population and the economy have both led to more consumption of energy. Pollution in the air is an important factor of damage to the environmental. In addition to this, it's essential to develop technologies that can precisely monitor pollutants and harmful gases. Gas sensors are very essential in many fields which include monitoring the environment, utilizing them in industry, food safety, and medical diagnostics[1, 2]. Nitrogen dioxide (NO_2) is one of the most concerning pollutants because of its strong smell and the probability of major health consequences even at extremely low concentrations, which are expressed in parts per million (ppm) or parts per billion (ppb)[3, 4]. Ammonia (NH_3) is a widespread hazardous gas that is created by industrial, agricultural, and organic decomposition systems. The chemical manufacturing is heavily used, especially in fertilizers. High concentration exposure is harmful to both human health and the environment since it produces extreme irritation and harm to the skin, eyes, and respiratory system. Therefore, it is crucial to create sensors that can detect ammonia at low concentrations with sensitivity and selectivity to ensure industrial and environmental safety[5–7]. Nanotechnology has provided the expansion of (small, highly) efficient gas sensors by increasing the surface area and developing the electronic properties of nanomaterials, thus enhancing sensor sensitivity[8, 9]. Various nanomaterials, such as SnO_2, ZnO, graphene, and TiO_2, have been used in gas sensing after being prepared and deposited onto electrodes using modern methods, such as distillation, printing, and spin coating. These sensors are widely used in environmental monitoring, medical diagnostics, the food industry, home safety, and military and industrial applications for detecting toxic and flammable gases, making them essential for protecting human health and the

environment[10, 11]. When the sensor is activated in air, oxygen molecules on the SnO_2 surface are adsorbed and capture electrons from the conduction band, resulting in the development of a greater potential barrier and a depletion layer at the grain boundaries, thus increasing the sensor's resistance. Metal oxide semiconductors for example SnO_2 are extensive used in gas sensing due to their high sensitivity and constancy[12]. The gases interact with the adsorbed oxygen and return electrons to the material when exposed to reducing gases, such as NH_3, further reducing the resistance and lowering the potential barrier. In contrast, oxidizing gases for instance NO_2 caused increasing the thickness of the depletion layer and raised the resistance. The change in the potential barrier height at the grain boundaries resulting from the surface interactions with the gas resulting in the change in the potential barrier is essentially the principle of sensitivity[13].

Semiconducting metal oxide sensors (MOS), for instance SnO_2 depended on changes in their electrical resistance when interacting with ideal gases. Research topic focuses on enhances selectivity, sensitivity, recovery, and response times. A sensor primarily contains a sensing layer and a transducer, both of which directly impact performance. While most conventional MOS sensors rely on a heater, room-temperature sensors have recently emerged, representing a significant step toward reducing power consumption and increasing detection efficiency down to ppb concentrations[14, 15]. An n-type metal oxide (SnO_2) is coupled with a p-doped (CuO), consisting of an internal potential barrier at the contact surface. Heterogeneous p-n junctions in p-doped MOS sensors significantly enhance gas detection performance during gas interaction and enable high sensitivity to rapid response, low concentrations, and low power consumption [16].

This study aimed to improve preparation parameters to enhance sensitivity, response speed, and selectivity toward NH_3 and NO_2 gases.

2. Experimental part

Pure tin oxide nanostructure thin films were deposited with tin oxide doped with copper using different volumetric ratios of copper solution (1,3,5) using chemical spray pyrolysis technique. Solutions of the materials were prepared from tin chloride ($SnCl_2.2H_2O$) with a molecular weight of 225.63 g/mol. This substance is a white powder which dissolves rapidly in water and is manufactured by (OXFORD LAB CHEM) with purity (99%), copper chloride ($CuCl_2$: $2H_2O$) and its molecular weight (170.48 g/mol) and manufactured by company (ALPHA CHEMIKA) with purity (99%). This solution was prepared at a molar concentration of 0.02 mol/L. The substrates were cleaned with distilled water and ethanol in an ultrasonic bath for 10 minutes to ensure that there was no contaminant on the surface. The solutions were sprayed on glass substrates with temperature 350 °C. The carrier gas is compressed air at a pressure of 1 bar was used with spraying processes was performed in alternating with period 5 seconds of spraying followed by 20 seconds pause, with a deposition rate of 2.5 ml/min. The thickness of the extracted thin films, which ranged from 350 to 450 nm, was determined using the optical method.

The optical properties were checked using ultraviolet-visible spectrophotometer. On the other hand, the structural and surface characteristics were analyzed by AFM-Atomic Force Microscopic, XRD, and SEM. Measuring the sensor response to ammonia (NH_3) and nitrogen dioxide (NO_2) gases at a concentration of 50 ppm under different temperatures was investigated using gas sensing properties. Furthermore, aluminum electrodes were deposited onto the films to evaluate the electrical performance.

3. Results and discussion

3.1. XRD analysis

The X-ray diffraction (XRD) patterns of pure and Cu-doped SnO_2 thin films with doping ratios of 1%, 3%, and 5% that were deposited on glass substrates using the chemical spray pyrolysis method at a precursor concentration of 0.02 M, are shown in Figure (1). The polycrystalline character of the deposited films is confirmed by the diffraction patterns of the undoped SnO_2 film, which show multiple distinct peaks corresponding to various crystallographic planes. The observed diffraction peaks are indexed to the (110), (101), (200), and (211) planes, located at diffraction angles of 2θ = 26.43°, 33.96°, 38.02°, and 51.82°, respectively, with a strong preferred orientation along the (110) plane. Comparison with the standard JCPDS card for SnO_2 (No. 41-1445) confirms that the films crystallize in the tetragonal rutile structure, in good agreement with previously reported results [17, 18]. With increasing Cu doping concentration, a noticeable reduction in the intensity of the SnO_2 diffraction peaks was observed, while the preferred orientation along the (110) plane was preserved, as shown in Figure (1). This behavior suggests that Cu inclusion causes a little decrease in crystallinity or the emergence of lattice instability. The Debye–Scherrer equation was used to calculate the average crystallite size (D) [19]:

$$D = 0.94\lambda/\beta cos\theta \quad (1)$$

The form factor is 0.94, the diffraction peak's full width at half maximum (FWHM) is β, the Bragg angle is θ, and the wavelength of the Cu Kα radiation source is (λ = 0.15405) nm. According to Table (1), the average size of crystallites decreased as the concentration of Cu increased, ranging from 6.42 to 5.09 nm. Furthermore, Cu doping does not alter the crystal structure of SnO_2 or create any new phases, hence the tetragonal rutile phase is unaffected by doping. Since the ionic radii of Cu^{2+} (0.69 Å) and Sn^{2+} (0.71 Å) are so comparable, Cu ions can replace Sn ions in the lattice, resulting in no extra diffraction peaks. According to earlier observations, Cu ions can occupy Sn sites within the SnO2 lattice through this substitutional doping mechanism without generating distinct CuO or Cu_2O phases[18].

3-2- AFM results

Figure (2): Atomic force microscopy (AFM) analyses of pure and Cu-doped tin oxide thin films with doping ratios of 1%, 3%, and 5% deposited on glass substrates at a temperature of 350°C and a molar concentration of 0.02 M. The images reveal a uniform grain distribution over the surface. In addition, the films are homogeneous and free of cracks.

The results also indicate that the surface topography of the doped films exhibits good crystalline regularity and high surface homogeneity, with grains uniformly distributed over the entire film surface. Furthermore, the Cu doping process led to a gradual reduction in both the surface roughness and the average particle size for all doped films. Table 1 summarizes the results obtained from the AFM measurements for the SnO_2 and Cu-doped tin oxide thin films.

Table 1
AFM results and crystal size of pure and Cu-doped SnO_2 films.

Sample	Crystallite size (D) (nm)	Roughness average (nm)	Average grain size (nm)
SnO_2	6.42	21.5	88.35
SnO_2: 1% Cu	6.04	11.9	63.7
SnO_2: 3% Cu	5.91	8.19	26.9
SnO_2: 5% Cu	5.09	3.73	9.1

3-3- SEM

Figure (3) shows the SEM micrographs and corresponding particle size distributions of pure SnO_2 and Cu-doped SnO_2 thin films. The pure SnO_2 film exhibits relatively larger, quasi-spherical nanoparticles with noticeable agglomeration, with particle sizes mainly distributed in the range of ~ 80–120 nm. Upon Cu incorporation (1% Cu), a significant reduction in the average particle size was observed, with a narrower size distribution (~ 50–90 nm) and improved particle dispersion. At higher Cu concentrations (3% Cu), the particle size distribution becomes broader, and partial agglomeration is re-observed. For the highest Cu content (5% Cu), the films exhibit a porous and rough surface morphology, with smaller primary nanoparticles embedded within larger interconnected agglomerates.

Overall, Cu doping effectively tailors the microstructure of SnO_2 thin films by initially reducing the grain size and enhancing uniformity at low dopant levels, whereas higher Cu concentrations induce increased defect density, phase segregation, and porosity. These morphological modifications are expected to increase the specific surface area and the density of grain boundaries, which are critical factors for enhancing gas sensing performance and optoelectronic response.

Figure (4) presents the cross-sectional image obtained by field-emission scanning electron microscopy (FESEM)..It is observed that the thickness of the SnO_2 thin films is approximately 390.4 nm.

3-4- EDS analysis

Figure (5) shows the qualitative analysis of pure and Cu-doped tin oxide thin films, where the presence of the main constituent elements, namely, tin (Sn) and oxygen (O), in addition to copper (Cu) used as the dopant, is clearly observed. This confirms the high purity of the prepared films and the absence of any extraneous elements within the detection limits of the measurement technique. It was observed that copper was not detected at the 1% doping level, which can be attributed to its concentration being below the detection limit of the analysis system. Furthermore, increasing the doping concentration leads to a noticeable increase in the copper content in the films.

The results also indicate that the weight percentage of tin increases, whereas that of oxygen decreases with increasing doping concentration, which results in an enhancement of the electrical conductivity of the films. Because oxygen limits the valence electrons of tin, increasing the ratio of tin to oxygen raises the density of free charge carriers, which enhances electrical conductivity. Additionally, Cu doping results in a decrease in oxygen content as well as an increase in copper and tin concentrations. This may be attributed to possible interactions between copper and tin in the presence of oxygen, which can modify the elemental distribution and promote the formation of structural defects, such as oxygen vacancies, playing an important role in enhancing the electrical properties of the films.

3.5. Optical properties

The absorbance as a function of wavelength for SnO_2 thin films and Cu-doped SnO_2 thin films with 1%, 3%, and 5% doping concentrations is shown in Figure (6). It is evident that when the concentration of copper doping increases, the absorbance drops. This behavior is attributed to the reduction in thin film thickness resulting from the increased copper content, which leads to a shorter optical path length within the deposited films and consequently lower absorbance. This result is in good agreement with those reported in Ref. [20, 21].

The results show that the direct bandgap value of undoped tin oxide before doping was approximately 3.73 eV, as shown in Fig. (7). After copper doping with three different concentrations (1%, 3%, and 5%), the direct bandgap values were found to be approximately (3.80, 3.83, and 3.88) eV, respectively, and this agreement with previous[22] .

The quantum confinement effect is responsible for the apparent rise in the energy band gap as the ratio of copper content increases. This disorder increase can be attributed to two possible factors: either copper incorporation generates energy levels near the conduction band, or the introduction of copper into the system leads to the formation of oxygen vacancies, which in turn create energy levels close to the conduction band[23, 24].

3.6. Hall effect measurements

The Hall effect measurements revealed that all pure and doped SnO_2 films prepared by the chemical spray pyrolysis exhibit n-type conductivity. The results also showed that the addition of different doping concentrations leads to a noticeable increase in charge carrier concentration, accompanied by an increase in mobility values compared to the undoped films. This behavior is attributed to the increase in average grain size and the decrease in grain boundary density with increasing copper (Cu) doping concentrations. Furthermore, the persistence of the negative sign of the Hall coefficient with increasing doping levels indicates that electrons are the dominant charge carriers and are responsible for the enhancement in electrical conductivity. Table (2) summarizes the Hall measurement results, including mobility, conductivity, Hall coefficient, and carrier type.

Table 2
Hall effect measurements of pure SnO_2 and Cu-doped SnO_2 films.

Sample	n $(cm)^{-3}$	R_H $(cm^{-3}C^{-1})$	σ $(Ω.cm)^{-1}$	μ $(cm^2V^{-1}s^{-1})$	Type of conductivity
SnO_2 pure	$-5.9 \times 10^{+16}$	$-1.04 \times 10^{+2}$	$1.3 \times 10^{+1}$	$1.4 \times 10^{+3}$	n-Type
Cu 1%	$-7.03 \times 10^{+15}$	$-8.8 \times 10^{+2}$	7.8×10^{-2}	$6.9 \times 10^{+1}$	n-Type
Cu 3%	$-6.1 \times 10^{+17}$	$-1.01 \times 10^{+1}$	7.7×10^{-1}	7.8	n-Type
Cu 5%	$-8.4 \times 10^{+16}$	$-7.4 \times 10^{+1}$	3.3×10^{-1}	$2.4 \times 10^{+1}$	n-Type

3.6. Gas-sensing measurements

3.6.1.NH_3 gas sensor

The response of nanostructured films pure SnO_2 and Cu-doped SnO_2 gas sensors with different doping ratios toward ammonia (NH_3) gas at a concentration of 50 ppm was investigated. Figures (8) illustrates the variation in sensitivity as a function of operating temperature for pure and Cu-doped SnO_2 thin films exposed to NH_3 gas. Ammonia is classified as a reducing gas, whereas tin dioxide is an n-type semiconductor. Therefore, upon exposure to NH_3, a decrease in the electrical resistance of the film occurs due to the increase in electron concentration in the conduction band, from which the sensitivity is calculated.

The highest sensitivity value for the pure SnO_2 film was 16.79% at an operating temperature of 25°C, with a response time of 32.4 s and a recovery time of 170.1 s. When the operating temperature was increased to 200°C, the sensitivity decreased to 5.65%, accompanied by a response time of 16.2 s and a recovery time of 76.5 s, as shown in Figure (9). These findings show that the sensitivity decreases with temperature, which is explained by the decreased interaction between the ammonia gas and the film surface at higher temperatures. Compared to the pure film, doping SnO_2 with 1% Cu resulted in a significant increase in sensitivity. The maximum sensitivity reached 19.12% at an operating temperature of 200°C, with a response time of 29.7 s and a recovery time of 95.4 s. However, increasing the Cu doping ratio to 3% resulted in a reduction in sensitivity to 8.4% at 200°C, with a response time of 25.2 s and a recovery time of 45 s, as presented in the table. At a higher doping level of 5% Cu, the sensitivity decreased significantly to approximately 1.1% at 200°C, with a response time of 21.6 s and a recovery time of 45 s, as shown in Table 3. It can be concluded that Cu doping enhances the sensitivity of SnO_2 thin films compared to the undoped film; however, the sensitivity decreases with increasing dopant concentration. This behavior can be explained by the interaction between NH_3 molecules and the adsorbed oxygen ions on the sensor surface, leading to the release of electrons into the conduction band and consequently a decrease in the electrical resistance of the sensor, according to the following reactions [25, 26]:

$$NH_3 + 3O_2^- (ads) \rightarrow 2N_2 + 6H_2O + 6e^- \quad (2)$$

$$NH_3 (ads) + 3O_2^- (ads) \rightarrow N_2 + 3H_2O + 3e^- \quad (3)$$

These reactions require activation energy, indicating that thermal energy must be supplied to facilitate the sensing process.

Table 3
Sensitivity values, response time, and recovery time of pure and copper-doped SnO_2 films with different doping ratios toward NH_3 gas at a concentration of 50 ppm.

Sample	Operating Temp. °C	Sensitivity %	Res. Time (s)	Rec. Time (s)
SnO_2-Pure	50	16.79	32.4	170.1
	100	3.12	25.2	90.9
	200	5.65	16.2	76.5
SnO_2: Cu 1%	50	1.13	26.1	133.2
	100	19.12	29.7	95.4
	200	5.86	28.8	88.2
SnO_2: Cu 3%	50	2.05	23.4	94.5
	100	2.66	29.7	68.4
	200	8.48	25.2	45
SnO_2: Cu 5%	50	1	22.5	94.5
	100	0.11	19.8	49.5
	200	1.1	21.6	45

3.6.2. NO_2 gas sensor

Figure (10) shows how a pure SnO_2 film's sensitivity varies with operating temperature. While prepared tin dioxide is an n-type semiconductor, nitrogen dioxide (NO_2) is an oxidizing gas. When the SnO_2 sensor is exposed to nitrogen dioxide gas, a surface chemical interaction occurs that results in electron withdrawal and an increase in electrical resistance, from which the sensitivity is calculated. The results show that the sensitivity of the pure SnO_2 film increases with increasing operating temperature, reaching its maximum value at 200°C, as listed in Table 4. For SnO_2 films doped with 1% copper, a significant enhancement in sensitivity was observed compared with the undoped film. The highest sensitivity reached 96.14% at an operating temperature of 200°C, with a response time of 33.3 s and a recovery time of 92.7 s, as shown in figure (11). In contrast, increasing the Cu doping concentration to 3% led to a noticeable reduction in sensitivity, and this decreasing trend continued when the doping level was increased to 5%, as shown in Table 4.

The temperature-dependent sensitivity behavior can be attributed to the establishment of equilibrium between oxygen adsorbed on the SnO_2 surface and atmospheric oxygen, which stabilizes the electrical conductivity. Subsequently, chemisorption of NO_2 gas occurs on the oxide surface, causing electron

transfer toward the surface and resulting in a change in conductivity and, consequently, an increase in sensitivity. The sensor response mechanism depends mainly on two factors [27]: the rate of surface chemical reactions on the grain boundaries and the diffusion rate of gas molecules within the oxide layer. The increase in sensitivity with operating temperature indicates that the interaction between NO_2 gas and the SnO_2 sensing films is a thermally activated process. Upon exposure to NO_2, gas molecules react with the oxygen species adsorbed on the surface, capturing electrons from the sensor and increasing its electrical resistance, as described by the following reactions [28]:

$$\mathrm{NO_2\,(g) + e^- \rightarrow NO^-\,(ads)}$$

4

$$\mathrm{NO_2\,(g) + O^-\,(ads) + e^- \rightarrow NO_2^-\,(ads) + 2O^{2-}\,(ads)}$$

5

Overall, the sensitivity results indicate the existence of an optimum operating temperature at which the sensor becomes active and exhibits maximum performance. Up to a certain point, the sensitivity rises with temperature, indicating that activation energy is needed to finish the interaction between oxygen ions and NO_2 gas molecules. In contrast, the sensor response at room temperature was found to be very weak.

Table 4
Sensitivity values, response time, and recovery time of pure and copper-doped SnO_2 films with different doping ratios toward NO_2 gas at a concentration of (50 ppm).

Sample	Operating Tem. (°C)	Sensitivity (%)	Response Time (s)	Recovery Time (s)
SnO_2-Pure	50	3.52	34.2	172.8
	100	5.75	22.5	94.5
	200	10.72	31.5	85.5
SnO_2: Cu 1%	50	49.93	29.7	132.3
	100	69.81	27	72
	200	96.14	33.3	92.7
SnO_2: Cu 3%	50	12.3	24.3	98.1
	100	14.87	28.8	88.2
	200	10.49	19.8	52.2
SnO_2: Cu 5%	50	6.49	21.6	94.5
	100	5.07	22.5	67.5
	200	3.2	24.3	78.3

Conclusion

This work confirms that spray pyrolysis is an effective and straightforward method for producing pure and Cu-doped SnO_2 nanostructured thin films with improved optical, electrical, and structural characteristics. By increasing crystallite and grain sizes and improving surface uniformity, copper doping significantly affects the film microstructure and increases the effective surface area. All films had n-type properties, and optical studies revealed a progressive rise in the band gap with increased Cu content, while electrical experiments showed increased conductivity and carrier concentration. With the highest sensitivity and selectivity for NH_3 and NO_2 gases, 1% Cu-doped SnO_2 films performed the best, according to gas-sensing studies. Sensing efficiency was reduced at higher doping concentrations (3% and 5%) due to a rise in inactive defects and carrier recombination. SnO_2: Cu thin films exhibit significant potential for industrial and environmental gas-sensing applications, especially those doped with 1% Cu. The results also establish an outline for subsequent research aimed at enhancing sensing efficacy at reduce operating temperatures or via integration with various nanomaterials.

Declarations

Conflicts of interest

The authors declare that there is no conflict of interest.

Author Contribution

All authors made significant and complementary contributions to this work. Abd alhameed A. Hameed was responsible for sample preparation and drafting the initial version of the manuscript. Ruaa H. Jasim contributed to the analysis and interpretation of the results J. F. Mohammad and Bial K. Al-Rawi supervised the project and critically reviewed the manuscript.

Acknowledgments

The authors would like to express their sincere gratitude to the Scientific Research Committee, College of Dentistry / University of Iraq, the College of Education for Pure Sciences / University of Anbar, and the Ministry of Education, for their valuable support that contributed to the completion of this work.

References

1. Amu-Darko, J. N. O., et al. (2023). Highly sensitive In_2O_3/PANI nanosheets gas sensor for NO_2 detection. *Journal of Environmental Chemical Engineering*, *11*(1), 109211.
2. Mohammad, J., et al. (2026). pH-Dependent growth and gas sensing properties of hydrothermally synthesized SnO_2 nanostructured films. *Applied Physics A*, *132*(3), 172.
3. Behera, B., & Chandra, S. (2018). Synthesis of WO_3 nanorods by thermal oxidation technique for NO_2 gas sensing application. *Materials Science in Semiconductor Processing*, *86*, 79–84.
4. Hathal, Y. R., et al. (2023). Influence of DC Magnetron Sputtering Power on Structural, Topography, and Gas Sensor Properties of Nb_2O_5/Si Thin Films. *Iraqi Journal of Physics*, *21*(3), 41–54.
5. Wang, J., et al. (2018). Enhanced NH_3 gas-sensing performance of silica modified CeO_2 nanostructure based sensors. *Sensors and Actuators B: Chemical*, *255*, 862–870.
6. AL-Jumaili, H. S. (2021). Preparation and characterization of In_2O_3-CuO nanocomposite thin films as NH_3 gas sensor. *Iraqi Journal of Science*, : pp. 2204–2212.
7. Hathal, Y. R., Ibrahim, I. M., & Khalaf, M. K. (2024). Effect of Substrate Temperature on Characteristics and Gas Sensing Properties of Nb_2O_5/Si Thin Films. *Iraqi Journal of Applied Physics*, *20*(2A), 271–277.
8. Al-Rawi, B. K., Shalaan, M. M., & Khalaf, M. K. (2025). Effect of Gold Dopant on Structure and Morphology Properties of Nanostructured Tungsten Oxide Thin Films. Nanoscience and Technology: An International Journal, 16(4).

9. Abduljabbar, Q. A., et al. (2025). Structural and optical properties of SnO_2/SnS nano-heterojunction thin films for gas sensor. *Journal of Materials Science: Materials in Electronics*, *36*(35), 2232.
10. Thabit, W. S., & Al-Rawi, B. K. (2023). The effect of atomization force on the structural properties of NiTi thin films. *International Journal Of Nanoscience* 22 (2).
11. Pippara, R. K., et al. (2021). Room temperature hydrogen sensing with polyaniline/SnO_2/Pd nanocomposites. *Micro and Nano Engineering*, *12*, 100086.
12. Mahmood, S. S. (2018). Characterization of (SnO_2) 1-x (TiO_2: CuO) x films as NH3 gas sensor. *Iraqi Journal of Physics*, *16*(39), 71–80.
13. Shivam, T., & Jha, R. K. (2026). Emerging 2D materials for hydrogen detection: mechanism, challenges, & opportunities. *Coordination Chemistry Reviews*, *549*, 217237.
14. Mehrabi, P. (2018). *Development of SnO_2/PEO nanofiber gas sensor for THC detection*. University of British Columbia.
15. Hussain, A. M., & Al-Rawi, B. K. (2024). Synthesis and characterizations of physical and antibacterial properties of the Ag nanoparticles by exploding of wire technique. *International Journal Of Nanoscience*, *23*(3), 2350075.
16. Bachhav, K., & Garde, A. S. Synthesis, characterization and fabrication of WO_3-CuO nanocomposite heterojunction thick film for detection of NO_2 gas.
17. Mohammed, J., & Ibrahim, I. M. (2025). Ultraviolet photodetectors based on nanostructured SnO_2 thin films/P-Si heterojunctions prepared by a hydrothermal method. *Jordan Journal of Physics*, *18*(3), 389–398.
18. Al-Rawi, B. K., & Ramizy, A. (2019). Modeling the vibrational properties of InSb diamondoids and nanocrystals using density functional theory. *Journal Of Inorganic And Organometallic Polymers And Materials*, *29*(3), 645–650.
19. Hameed, A. A. A., Mohammed, J., & Ibrahim, I. M. (2025). Study the effect of different pH values on the nanoparticle shape of ZnO films prepared by hydrothermal method. in AIP Conference Proceedings. AIP Publishing LLC.
20. Meteab, S. M., & Mohammad, J. (2023). Effect of Cu-Doping Levels on the Structural and Optical Properties of SnO_2 Thin Films Prepared by Chemical Spray Pyrolysis. *Revue des Composites et des Materiaux Avances*, *33*(5), 311.
21. Kathalingam, A., et al. (2018). Analysis of Sn concentration effect on Morphological, Optical, Electrical, and photonic properties of Spray-coated Sn-doped Cdo Thin Films. *Coatings*, *8*(5), 167.
22. Abbas, N. K. A., & Shaker, D. S. (2024). Study the Effects of Pure Tin Oxide Nanoparticles Doped with Cu, Prepared by the Biosynthesis Method, on Bacterial Activity. *Baghdad Science Journal*, *21*(11), 3543–3553.
23. Rzooqi, M. A., et al. (2025). AP0976 Characterization of Nanocomposites SnO_2: Cu for Gas Sensing Applications. *Iraqi Journal of Applied Physics*, *21*(3), 310–316.

24. Siva, J. V., Tripathy, S. K., & Ramalingeswara, R. A. (2020). Study of the structural, optical, dielectric and magnetic properties of copper-doped SnO_2 nanoparticles. *Journal of Electronic Materials*, *49*(6), 3540–3554.
25. Yang, C., Zhang, H., & Zhang, H. (2025). Preparation and mechanism study of highly sensitive NH_3 gas sensor based on Au-modified CdS nanoparticles. *Applied Surface Science*, *680*, 161389.
26. Su, P. G., Wang, C. C., & Zhang, K. F. (2025). Room-temperature NH_3 gas sensor based on Ag-PPy core-shell nanowires. *Sensors and Actuators A: Physical*, : p. 116867.
27. Pan, Z., et al. (2025). Novel metal oxides partially derived perovskite-structured hydroxides for room temperature trace NO_2 gas sensors under UV irradiation. *Talanta*, *286*, 127449.
28. Cruz Lozada, J. A., et al. (2025). High-sensitivity NO_2 gas sensor: exploiting UV-enhanced recovery in a hexadecafluorinated iron phthalocyanine-reduced graphene oxide. *ACS omega*, *10*(3), 2809–2818.

Figures

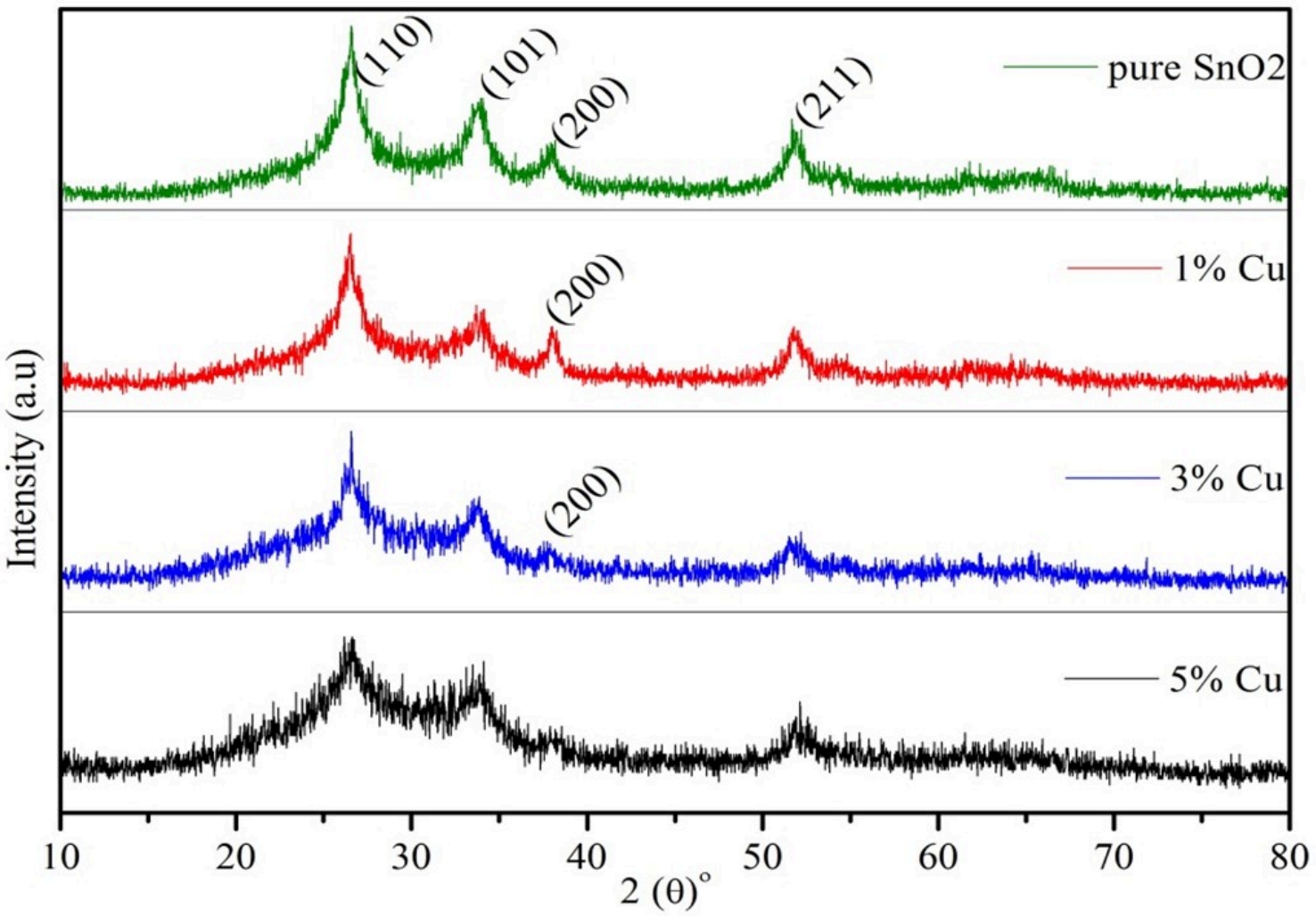


Figure 1

XRD patterns of pure and Cu-doped SnO_2 thin films at different copper doping concentrations.

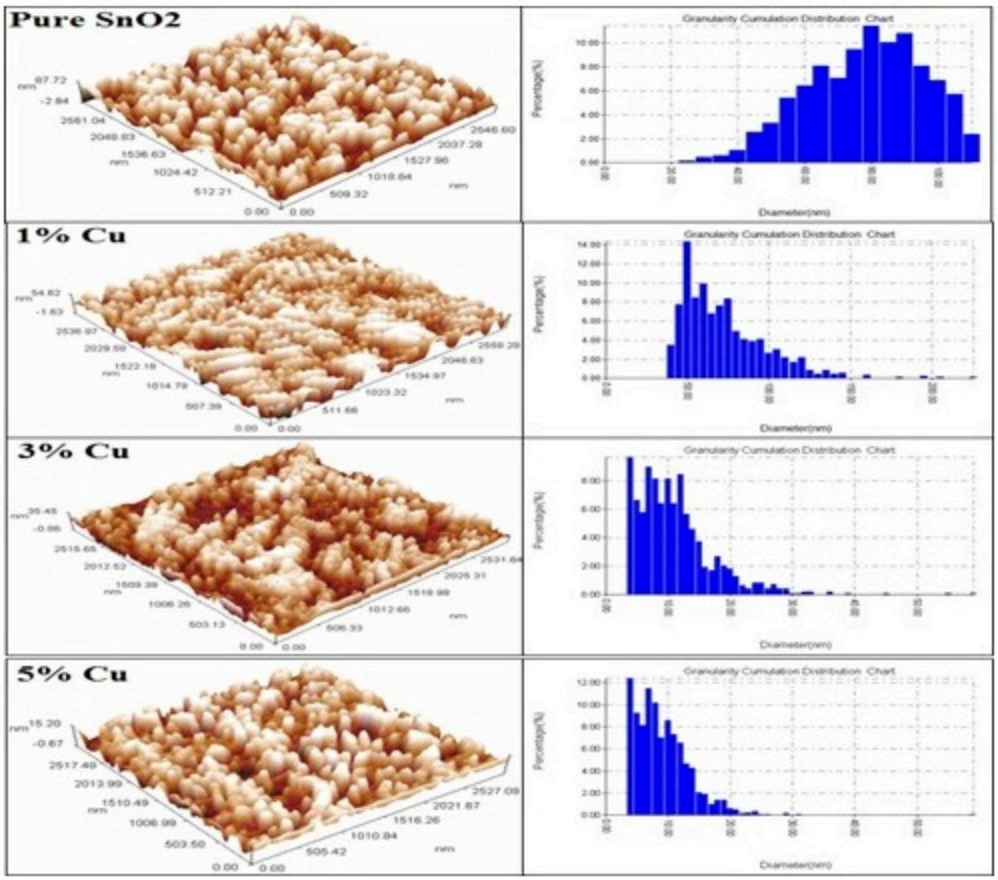


Figure 2

AFM images of pure and Cu-doped SnO_2 thin films with different doping concentrations, 1%, 3%, and 5% .

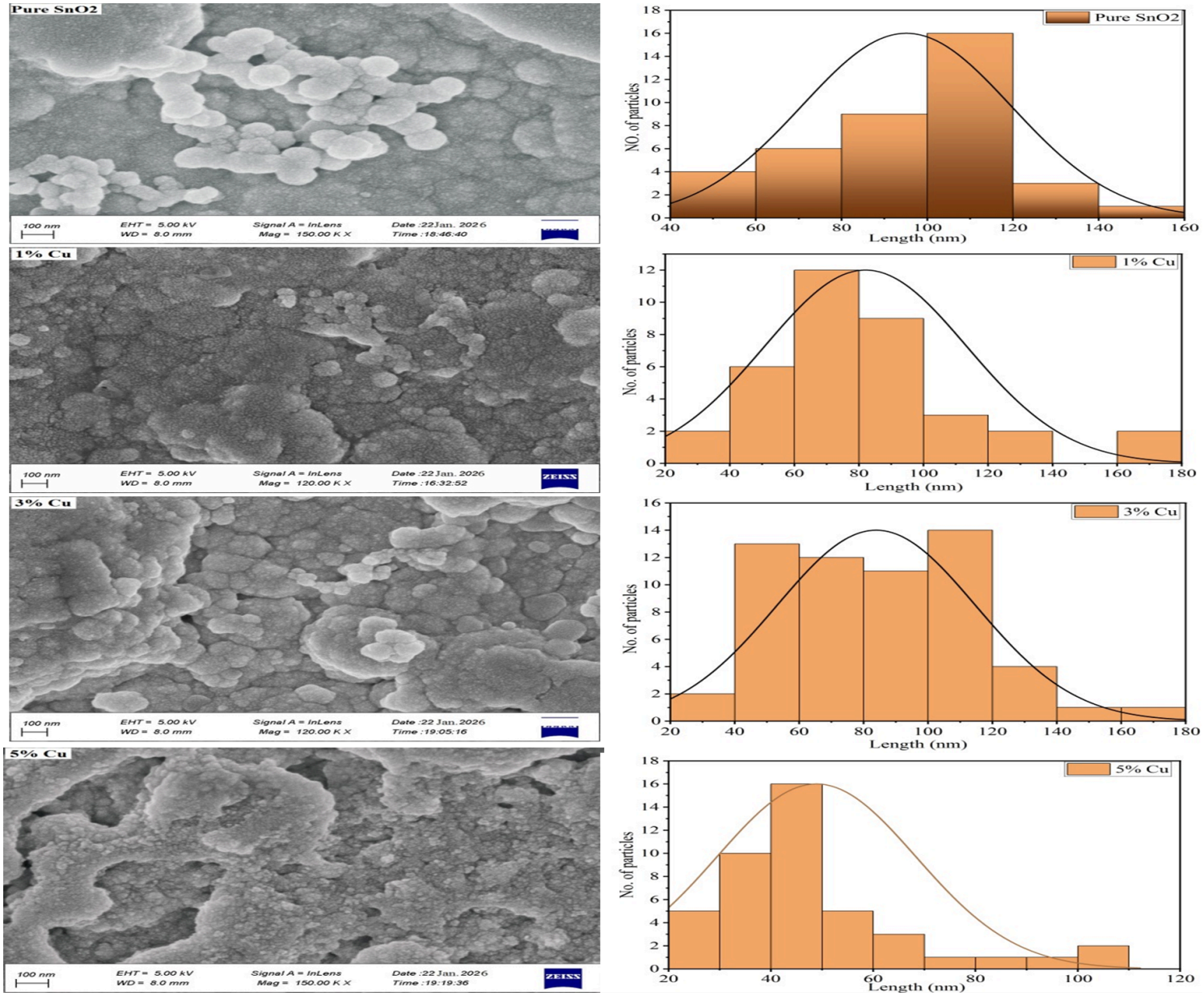


Figure 3

SEM images of pure and copper-doped SnO_2 films .

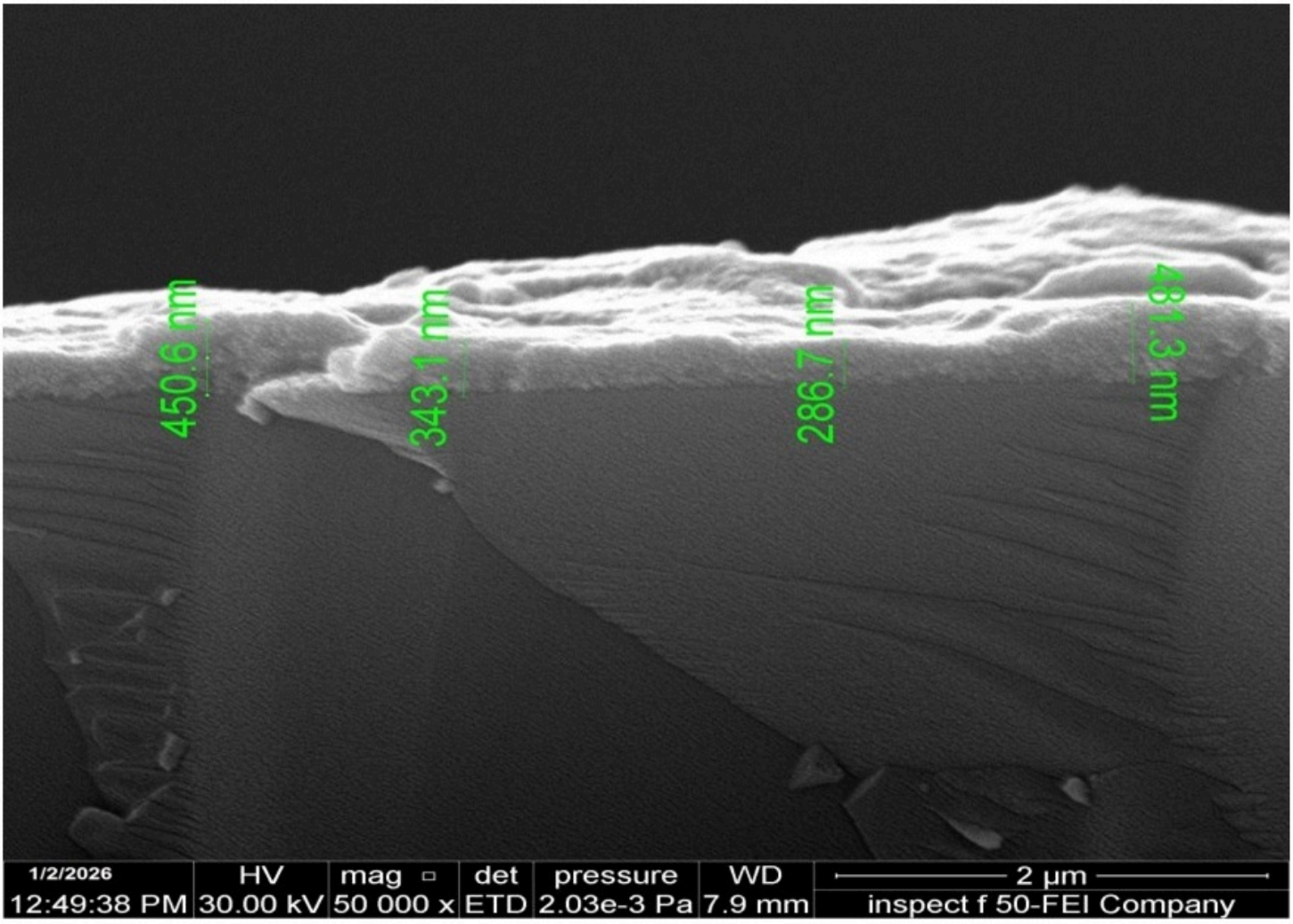


Figure 4

Cross-sectional FESEM image of pure SnO_2 films.

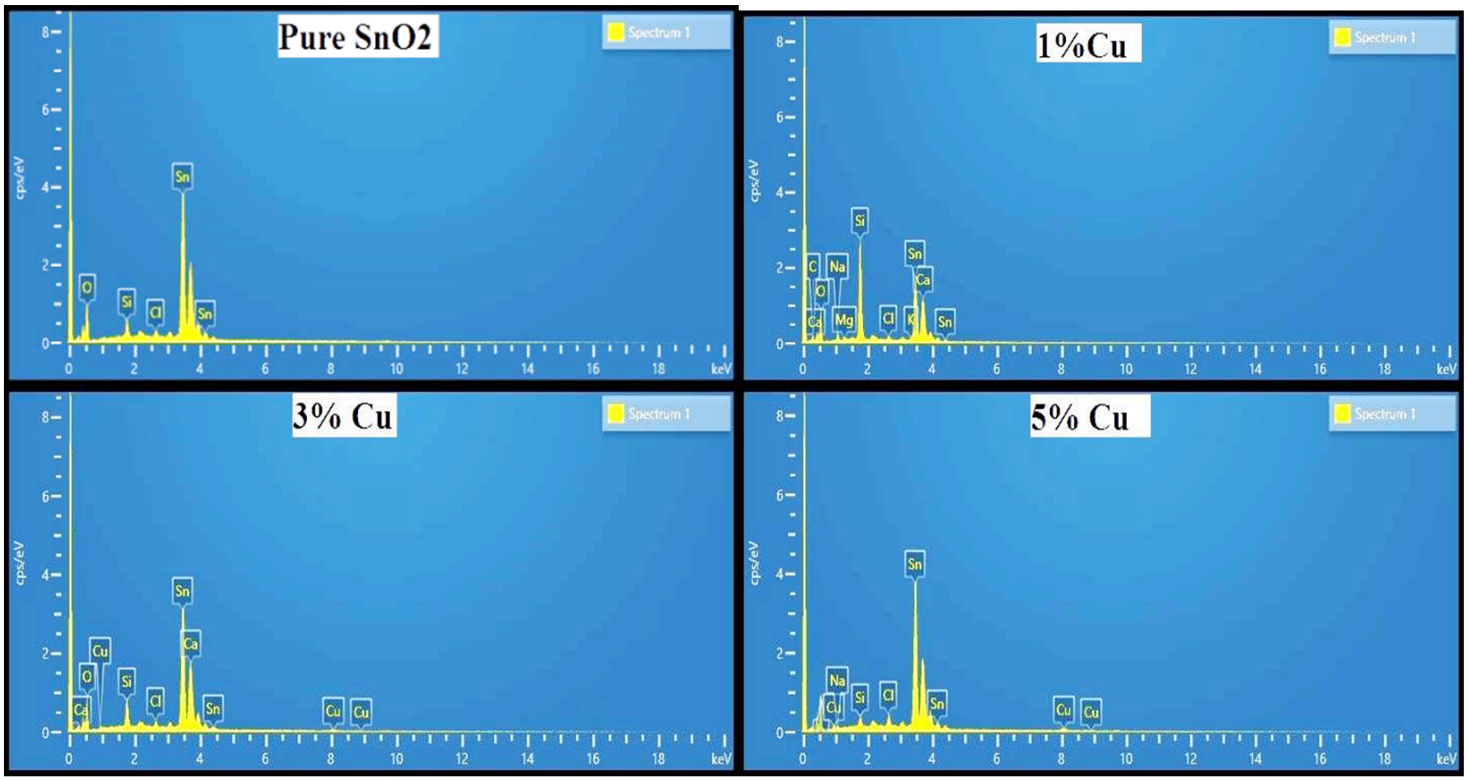


Figure 5

EDX images of pure and copper-doped (SnO_2) films at percentages of 1%, 3%, and 5%.

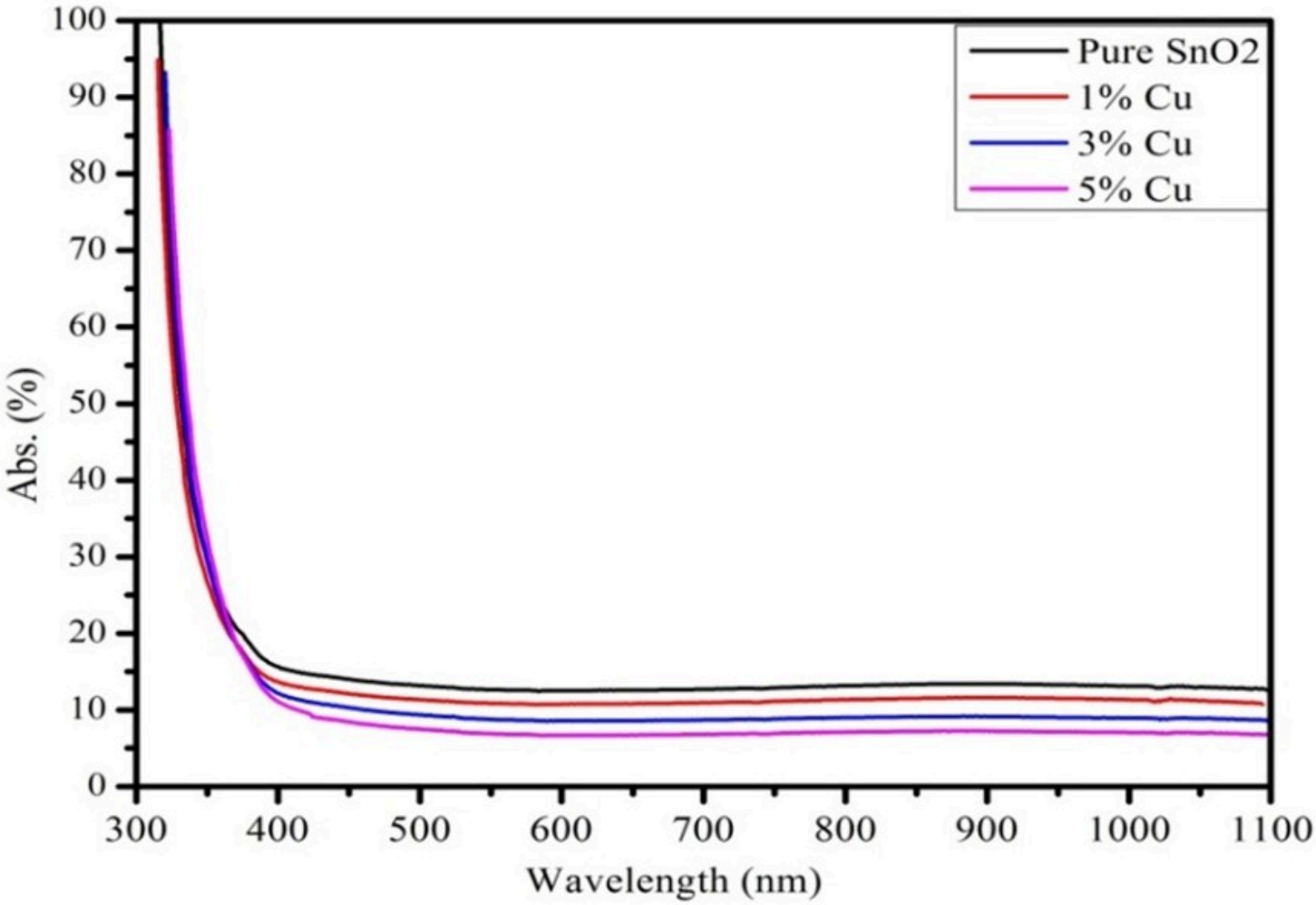


Figure 6

Absorbance of pure SnO_2 and Cu-doped SnO_2 (Cu: 1,3,5 %) films.

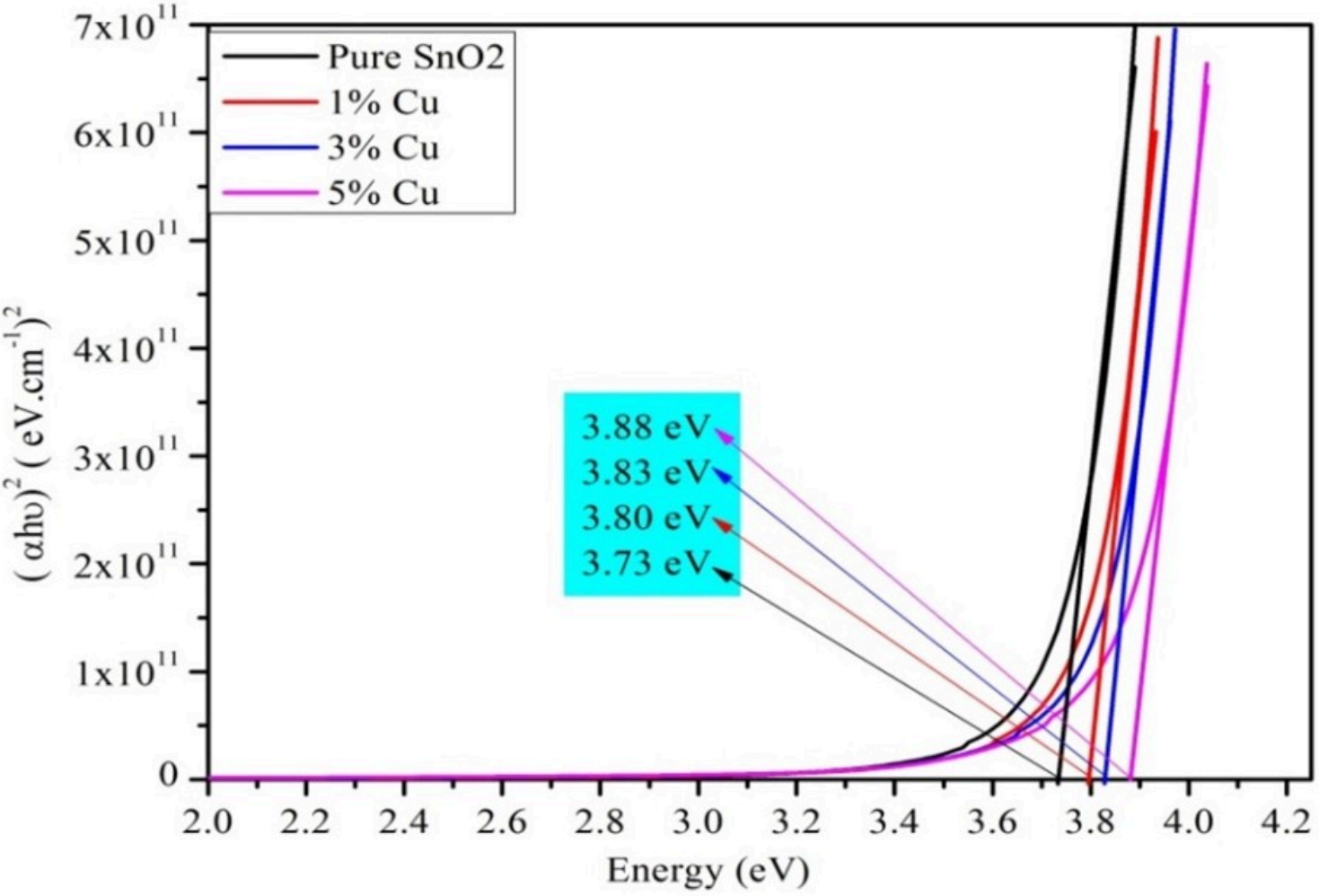


Figure 7

Optical energy gap of pure SnO_2 and Cu-doped SnO_2 films

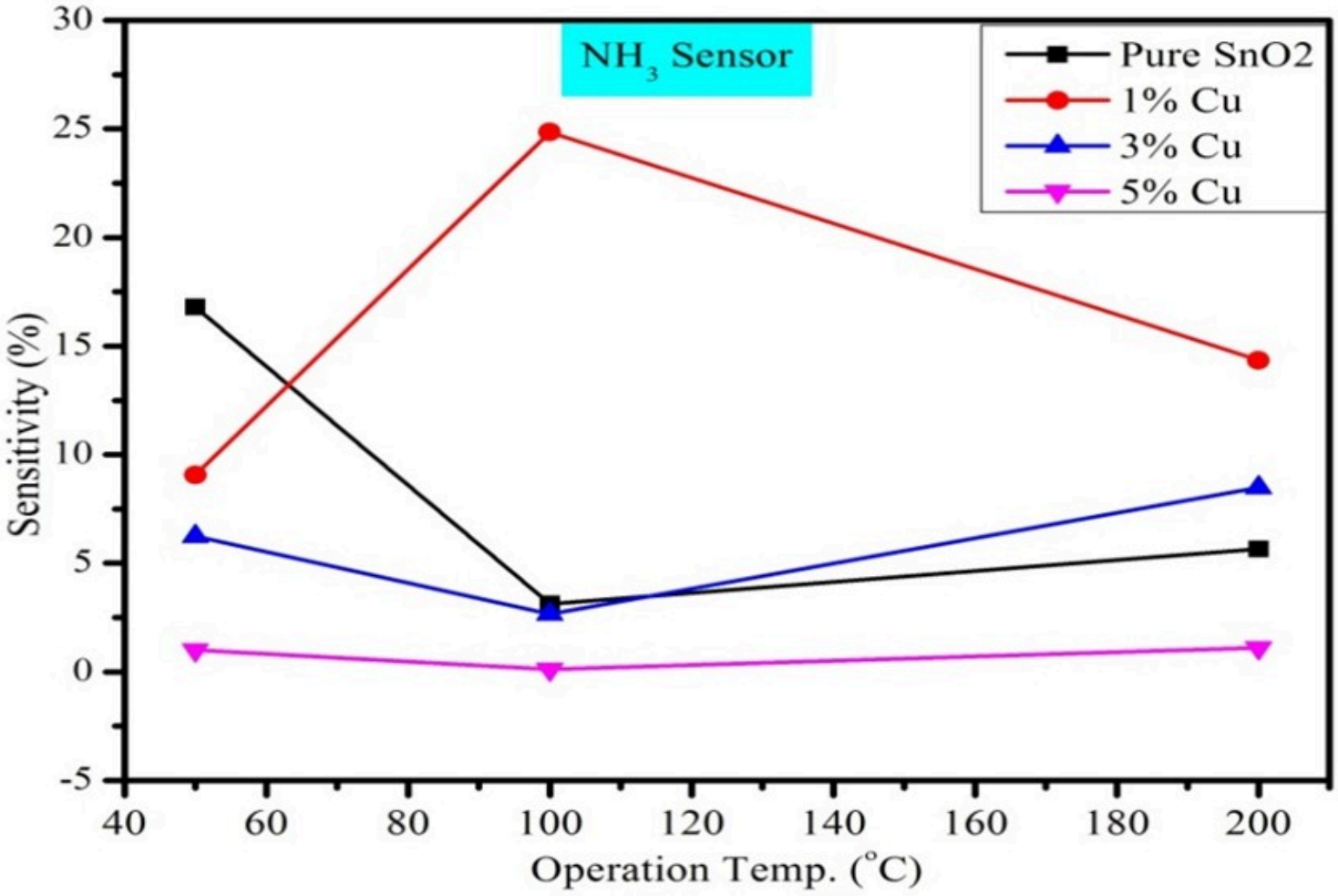


Figure 8

Variation in sensitivity with operating temperature for SnO_2 thin films, both pure and Cu-doped, with varying doping ratios (1%, 3%, and 5%) toward NH_3 gas at a 50 ppm concentration.

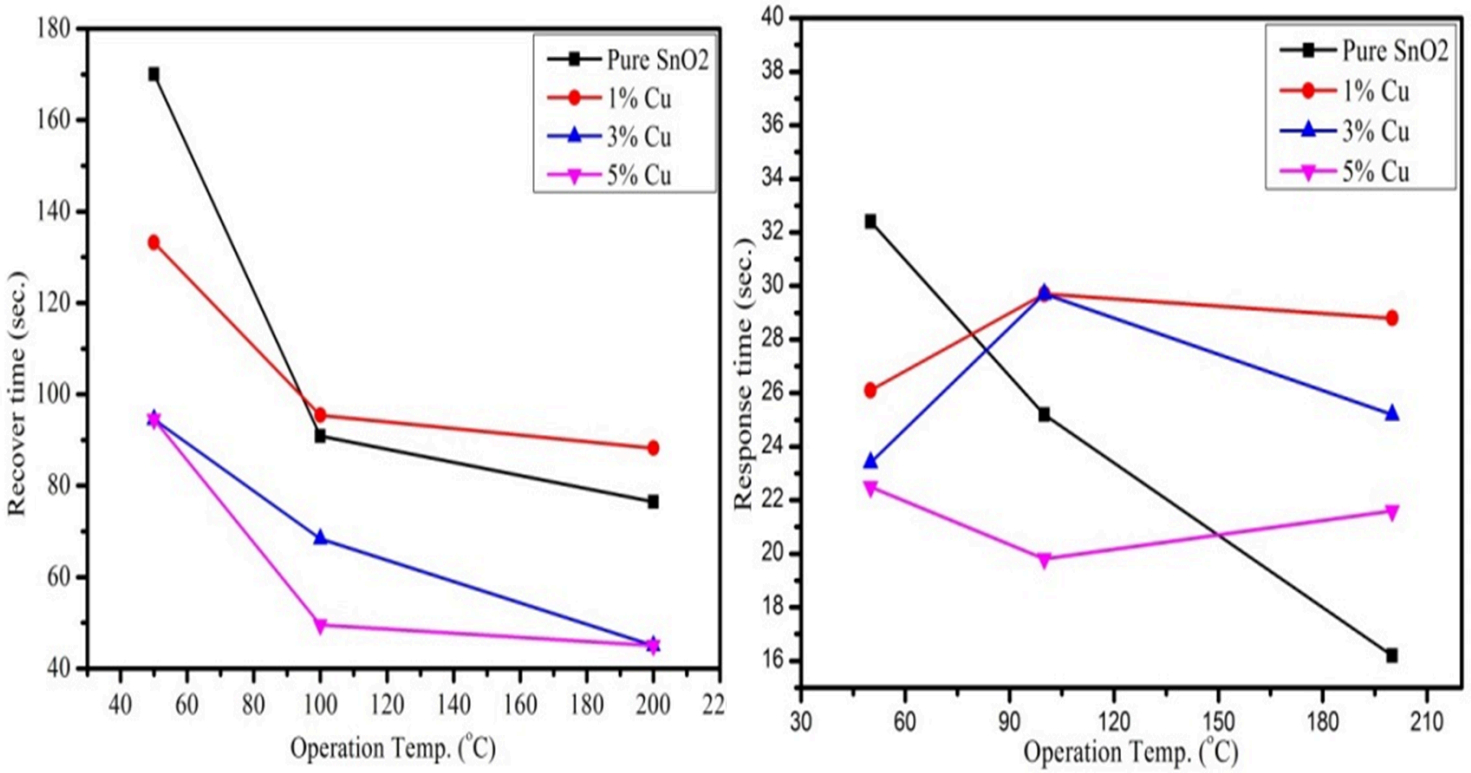


Figure 9

Changes in response and recovery times with temperature for pure and copper-doped tin oxide films.

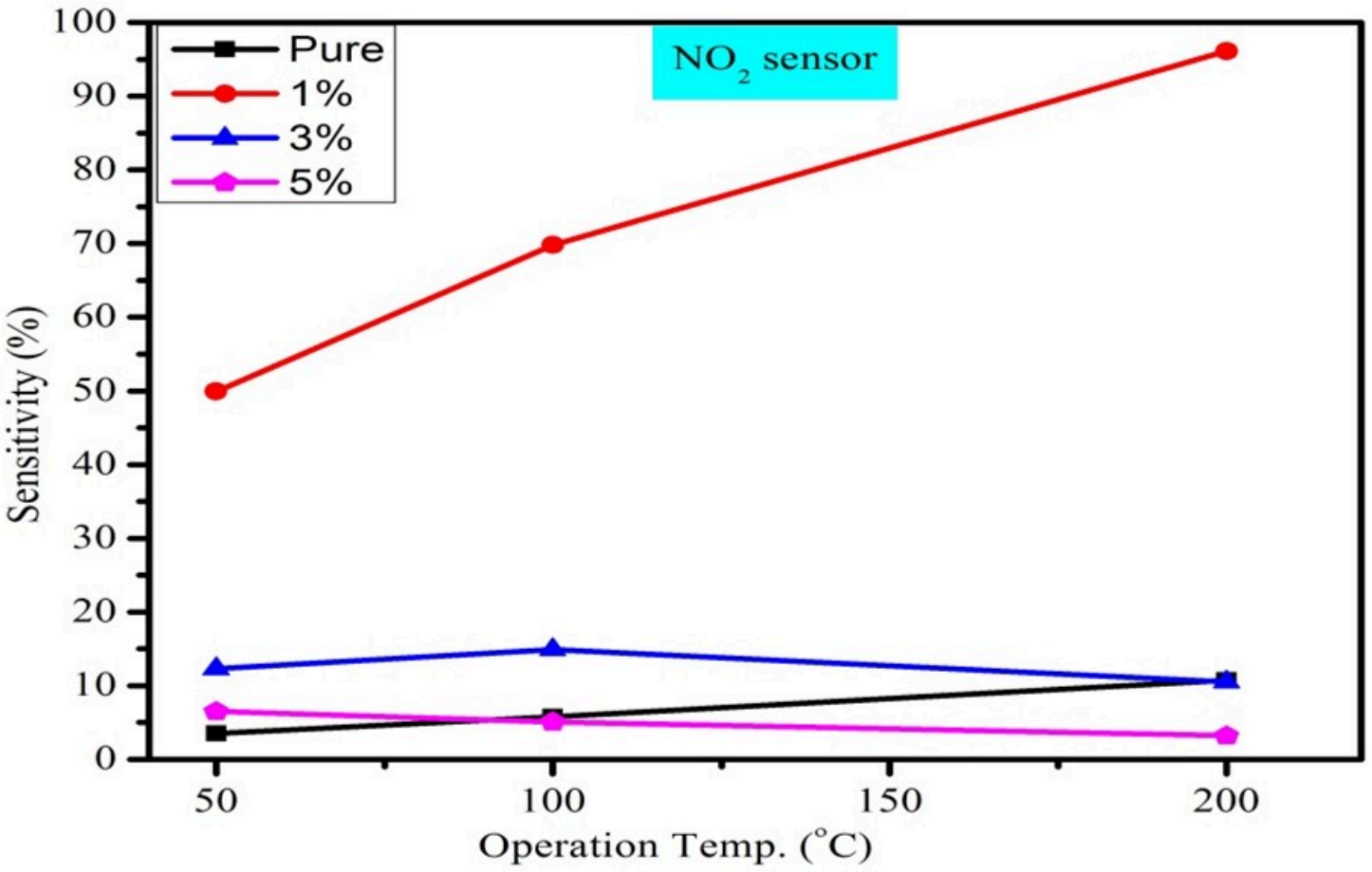


Figure 10

Variation in sensitivity with operating temperature for pure and Cu-doped SnO_2 thin films toward NO_2 gas at a 50 ppm concentration.

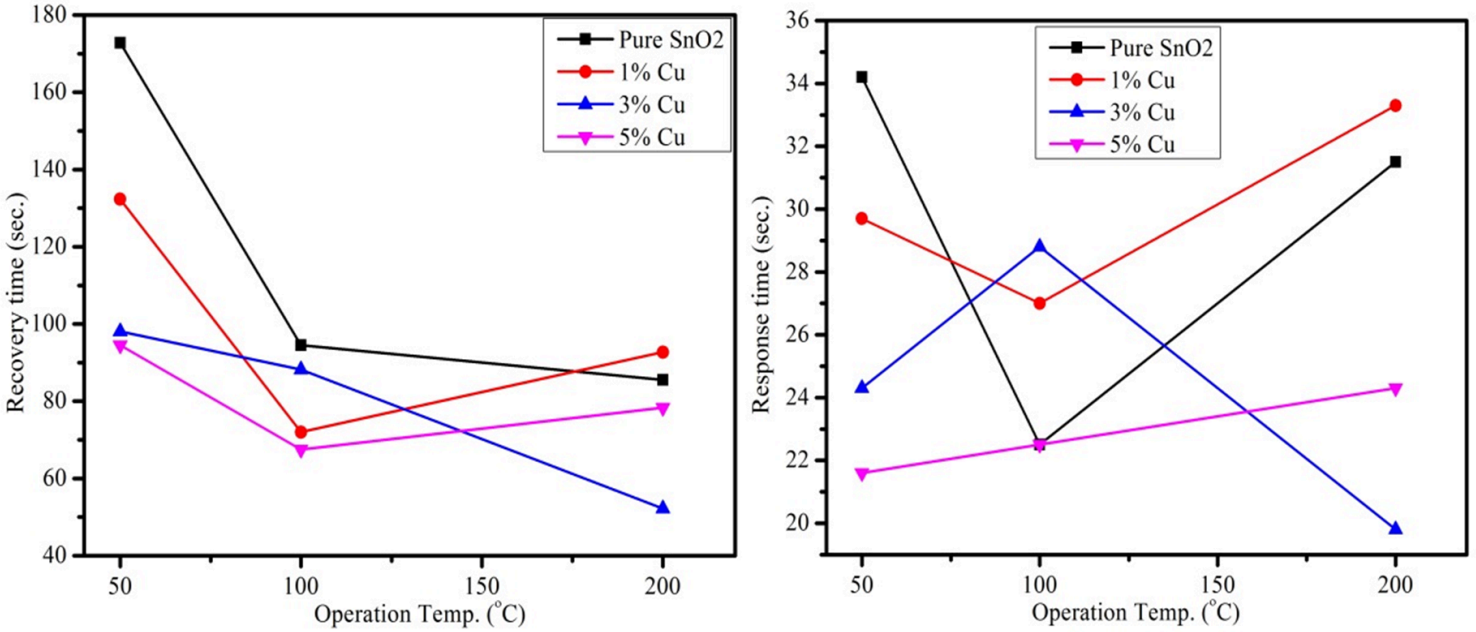


Figure 11

Changes in response and recovery times with temperature for pure and copper-doped tin oxide films.